

Conductance distribution in disordered quantum wires: crossover between the metallic and insulating regimes.

Victor A. Gopar and K. A. Muttalib

Department of Physics, University of Florida, P.O. Box 118440, Gainesville, FL 32611-8440

P. Woelke

Institut für Theorie der Kondensierten Materie, Universität Karlsruhe, Karlsruhe, Germany and

Institut für Nanotechnologie, Forschungszentrum Karlsruhe, Karlsruhe, Germany.

We calculate the distribution of the conductance $P(g)$ for a quasi-one-dimensional system in the metal to insulator crossover regime, based on a recent analytical method valid for all strengths of disorder. We show the evolution of $P(g)$ as a function of the disorder parameter from an insulator to a metal. Our results agree with numerical studies reported on this problem, and with exact analytical results for the average and variance of g .

PACS numbers: 73.23.-b, 71.30., 72.10.-d

I. INTRODUCTION

The study of electronic transport in quantum mesoscopic disordered systems has been a topic of interest for a long time [1, 2]. Due to the random positions of the impurities in such systems, quantum interference effects give rise to strong fluctuations in the conductance from sample to sample. These effects can be observed in a single disordered sample by changing, for example, the applied magnetic field [3, 4], since this is similar to a change in the impurity configuration of the sample. As a consequence of these fluctuations a statistical study of the conductance is required.

Many efforts have been made in order to have a complete statistical description of the conductance in the three different regimes of transport [1]: metallic ($\xi \ll L$), where ξ is the localization length and L the typical size of the system, insulating ($\xi \gg L$) and crossover ($\xi \sim L$). It is known that in the metallic regime the distribution of the conductance $P(g)$ is Gaussian, so the first and second moments, i.e., the average $\langle g \rangle$ and the variance $\text{var}(g)$ are enough to describe $P(g)$. It turns out that in the deeply metallic regime $\text{var}(g)$ is a pure number independent of the details of the system known as the universal conductance fluctuations, depending only on the presence or absence of time reversal symmetry and spin-rotational symmetry [5]. In the opposite regime of transport (insulating regime), the distribution of g is log-normal, which means that $\ln g$ follows a Gaussian distribution.

The intermediate regime of transport between the metallic and insulating regimes can be reached, for example, by increasing the disorder in a metallic sample. As the disorder is increased the conductance fluctuations grow in such way that $\text{var}(g)$ becomes of the same order as $\langle g \rangle$. In this case, the first two moments are no longer enough to describe $P(g)$. In fact, the full distribution of g is needed in order to have a good statistical characterization of the electronic transport. However, not much is known about the distribution of the conductance in the crossover regime, even in the case of a simple geometry like a quasi-one-dimensional system or quantum wire ($L \gg W$, where L is the length and W is the width of the system), where a smooth transition from the metallic to the insulating regime exists.

There are a number of numerical simulations in the intermediate regime which show a broad asymmetric distribution of g with a plateau for values of $g < 1$ and a strong decay for $g > 1$ [6, 7, 8, 9, 10]. Also, these numerical results have shown an interesting qualitatively similar behavior of $P(g)$ for quasi one, two and three dimensional systems [7, 8, 9, 10].

With respect to analytical results in the crossover region, the first two moments of the distribution of the conductance have been calculated, in fact, for all values of disorder for quasi one dimensional systems, using the supersymmetric non-linear sigma model (model) [12, 13]. For the complete distribution $P(g)$ beyond the metal and insulator limits, a systematic method has recently been developed by two of us [14]. Using this method, we were able to calculate $P(g)$ for quasi-one-dimensional systems near the crossover regime, approaching on the insulating side. It was predicted that on the insulating side $P(g)$ follows a "one-side" log-normal distribution cut off by a Gaussian for $g > 1$. Numerical calculations have shown a cutoff at $g = 1$ in the crossover and insulating regimes [8, 9, 10] and a "one-side" log-normal distribution for $g < 1$, in the insulating region [10, 11]. The method reproduces other well known insulating

Present address: 23, rue du Loess, F-67037 Strasbourg Cedex (France)

and metallic limits. For example, using the results of [14], Fig. 1 shows the average and variance of g as a function of the disorder parameter $\gamma = \gamma L$; the first two moments agree quantitatively well with those from the model, in the metallic and insulating limits. In Fig. 2, $P(g)$ is plotted for a metal and insulator case, using again the results of [14], which shows that the two limits are well captured by the method. However, the crossover regime is qualitatively correct only on the metallic and insulating sides, suggesting that the approximations made in [14] are not as good for the complete crossover region. Indeed, numerical simulations have shown that the drop in $P(g)$ at $g > 1$ appears to be exponential [9, 10], as opposed to the Gaussian cutoff predicted in [14]. It is therefore important to improve the approximations made in [14] in order to obtain a better description of the crossover regime.

In this work we calculate the distribution of the conductance in the crossover regime using the proposed method in [14] with some improvements. We show how $P(g)$ changes from a broad highly asymmetric "one-sided" log-normal distribution on the insulating side of the crossover regime to a Gaussian-like distribution on the metallic side of the crossover regime, as function of the disorder γ . The distribution at the crossover regime agrees with numerical results, except exactly at $g = 1$, which may be due to the existence of a singularity [10, 15] which might make our approximations less accurate.

II. SCATTERING APPROACH AND DMPK EQUATION

In order to study the conductance, we will use the scattering approach to electronic transport, in which the (dimensionless) conductance is given in terms of the transmission eigenvalues T_n by

$$g = \frac{\sum_{n=1}^N T_n}{N}; \quad (1)$$

where N is the number of channels or transverse modes of the wire. Due to the random positions of the impurities in a disordered sample, the eigenvalues T_n fluctuate from sample to sample and the distribution of g is given in general by $P(g) = \frac{1}{N} \sum_{i=1}^N \delta(g - T_i)$, where $\langle \dots \rangle$ indicates the average with the joint probability distribution of the transmission eigenvalues $p(fT_n, g)$.

For a mesoscopic quasi one-dimensional quantum wire, the evolution equation for the distribution $p(fT_n, g)$ as a function of the length of the system is given by the DoroKhov-Mello-Pereyra-Kumar (DMPK) equation [16]. For systems without time reversal invariance or unitary symmetry, which is the case that we study here, the DMPK equation can be written as

$$\frac{1}{L} \frac{\partial p(\cdot)}{\partial L} = \frac{1}{N} \sum_{n=1}^N \frac{\partial}{\partial T_n} [n(1 - T_n) J(\cdot)] \frac{\partial p(\cdot)}{\partial T_n J(\cdot)}; \quad (2)$$

where

$$J = \sum_{i=1}^N \sum_{j=i+1}^N T_i T_j; \quad (3)$$

$n = (1 - T_n)/T_n$ and l is the mean free path. The solution of the DMPK equation has been found by Beenakker and Rejzai [17] for all degree of disorder and it is given by

$$p(fx_i, g) = C \prod_{i < j}^N \left(\frac{\sinh^2 x_j - \sinh^2 x_i}{\sinh^2 x_i} \right) \prod_{i=1}^N \sinh 2x_i \det_{0}^{Z-1} e^{k^2 s = 4N} \tanh(k=2) k^{2m-1} P_{(ik-1)/2}(\cosh 2x_n); \quad (4)$$

where the x_i 's are related with the T_i 's by $T_i = \sinh^2 x_i$ or with the transmission eigenvalues by $T_i = 1/\cosh^2 x_i$; C is a normalization factor and $P_{(ik-1)/2}$ is a Legendre function.

Using the Fourier representation of the δ -function, the distribution of the conductance is given in general by

$$P(g) = \frac{1}{Z} \int_{-1}^1 \frac{d}{2} \prod_{i=1}^N dx_i \exp \left(i \sum_{i=1}^N g \frac{1}{\cosh^2 x_i} \right) p(fx_i, g) \quad (5)$$

with $p(fx_i, g)$ given by Eq. (4). The calculation of $P(g)$ from Eq. (5) involves a nontrivial N -fold integration.

III. FEATURES OF THE CURRENT METHOD

In the metallic regime, where the transmission eigenvalues $T \ll 1$ contribute significantly to the conductance, the ϵ_n 's ($\epsilon_n = (1 - T_n) = T_n$) are very close to each other and a continuum density for ϵ_n can be assumed. In this approximation the universal conductance fluctuations can be derived. On the other hand, in the insulating regime, the ϵ_n 's are much larger than the unity (small transmission) and separated exponentially. In this case, the lowest eigenvalue gives the most important contribution to the conductance and within this approximation the log-normal distribution for g can be derived. But none of these approximations can describe the crossover regime where the eigenvalues are neither very close to each other, nor exponentially separated. We will see, however, that it is possible to study $P(g)$ in the crossover region by making systematic corrections from the metal and insulating regimes.

In order to calculate the distribution $P(g)$ in the crossover regime, we propose, following [14], to separate out the two lowest eigenvalues x_1, x_2 , treating the rest as continuum. In [14] only the lowest eigenvalue x_1 was separated out. We will see that by separating out one additional eigenvalue we can go beyond the region studied in [14]. In the following we give a brief description of the important features of the current method in order to calculate $P(g)$.

The general solution of the DMPK equation (4) can be simplified for the cases $L \gg N \gg 1$ (metal) and $L \gg N \gg 1$ (insulator). In these cases the integral over k can be calculated analytically and the determinant is given, for example in the metallic regime, by a product of the difference of the square eigenvalues [17]. The solution for both metallic and insulating regimes can be written as:

$$p(fx_1g) = \frac{1}{Z} \exp[-H(fx_1g)] \quad (6)$$

with

$$H(fx_1g) = \sum_{i < j}^N u(x_i; x_j) + \sum_i^N V(x_i) \quad (7)$$

The $H(fx_1g)$ function can be interpreted as the Hamiltonian of N charges at the positions x_i with a two body interaction given by $u(x_i; x_j)$ and confinement potential $V(x_i)$. Those terms are given by

$$u(x_i; x_j) = \frac{1}{2} \ln |j \sinh^2 x_j - \sinh^2 x_i| - \frac{1}{2} \ln |x_j^2 - x_i^2| \quad (8)$$

$$V(x_i) = \begin{cases} \frac{1}{2} x_i^2 & \text{(metal)} \\ \frac{1}{4} \ln(x_i \sinh 2x_i) & \text{(insulator)} \end{cases} \quad (9)$$

The parameter β ($= \beta L$) is given by $\beta = N/L$ in quasi-one-dimension. $\beta \ll 1$ and $\beta \gg 1$ correspond to the metallic and insulating limits, respectively. $\beta \approx 1$ is the crossover regime. We can see from Eq. (9) that the one body potential $V(x_i)$ in the insulating regime differs by a logarithmic term from the corresponding $V(x_i)$ for a metal. In the localized regime the transmission is very small, i.e. $x_i \gg 1$ (since $T = 1/\cosh^2 x$) and then the logarithmic term is negligible compared to the other terms of $V(x_i)$. This means that the solution in the metallic regime might be used for the insulating regime as well. Therefore, we will assume that the solution in the metallic regime is also valid for the intermediate regime. We remark that it is not always possible to write the general solution $p(fx_1g)$, Eq. (4), in the form Eqs. (6-7). However, we will check the validity of our approximations by comparing the average and variance of g with the respective exact results from the model for those quantities [13].

Using Eqs. (5) and (6), the distribution of the conductance can be written as

$$P(g) = \frac{1}{Z} \int_0^\infty \frac{dx_1}{2} \exp[-i g x_1] \prod_{i=1}^N \frac{1}{\cosh^2 x_i} H(x_i) \quad (10)$$

where Z is a normalizing factor. In order to calculate the distribution of g , as mentioned before, we start by separating out the two lowest eigenvalues x_1 and x_2 in $H(x)$, Eq. (7):

$$H = H_{1,2} + \sum_{3 \leq i < j}^N u(x_i; x_j) + \sum_{3 \leq i}^N V(x_i) \quad (11)$$

with

$$H_{1,2} = u(x_1; x_2) + \sum_{3 \leq i}^N u(x_1; x_i) + \sum_{3 \leq i}^N u(x_2; x_i) + V(x_1) + V(x_2) \quad (12)$$

Now we make the continuum approximation:

$$H(x_1; x_2; x_3; \rho(x)) = V(x_1) + V(x_2) + \int_{x_3}^{\infty} dx \rho(x) u(x_1; x) + \int_{x_3}^{\infty} dx \rho(x) u(x_2; x) \\ + \frac{1}{2} \int_{x_3}^{\infty} dx \int_{x_3}^{\infty} dx^0 \rho(x) u(x; x^0) \rho(x^0) + \int_{x_3}^{\infty} dx \rho(x) V(x); \quad (13)$$

where we have introduced the density of eigenvalues $\rho(x)$ which has to be calculated in a self-consistent way and subject to the conditions $\rho(x) > 0$ and $\int_{x_3}^{\infty} \rho(x) dx = N/2$.

Defining the "free energy" F as

$$F(x_1; x_2; x_3; \rho(x)) = 2H(x_1; x_2; x_3; \rho(x)) + i \left[\frac{1}{\cosh^2(x_1)} + \frac{1}{\cosh^2(x_2)} + \int_{x_3}^{\infty} \frac{\rho(x)}{\cosh^2 x} \right]; \quad (14)$$

the distribution $P(g)$ can now be written as a functional integration:

$$P(g) = \frac{1}{Z} \int_{x_1}^{\infty} \frac{dx_1}{2} e^{i g} \int_{x_1}^{\infty} dx_2 \int_{x_2}^{\infty} dx_3 \int_{x_3}^{\infty} D[\rho(x)] e^{-F(x_1; x_2; x_3; \rho(x))}; \quad (15)$$

As in [14], in order to find the density $\rho(x)$ self-consistently, we minimize the free energy by taking the functional derivative: $\delta F(x_1; x_2; x_3; \rho(x))/\delta \rho(x) = 0$, which gives the following integral equation for the saddle point density $\rho_{sp}(x)$:

$$\int_{x_3}^{\infty} dx^0 u(x; x^0) \rho_{sp}(x; x^0) = u(x; x_1) + u(x; x_2) + \frac{i}{\cosh^2 x} + V(x); \quad (16)$$

The above integral equation can be solved when the lower limit goes to zero. In this case, the integral can be symmetrically extended to negative values which allows one to invert the kernel and obtain $\rho_{sp}(x)$. For the non-zero limit, we calculate $\rho_{sp}(x)$ using the following "shift approximation". In terms of the eigenvalues ϵ and ϵ^0 , the interaction term in H , Eq. (8), can be written as:

$$u(\epsilon; \epsilon^0) = \frac{1}{2} [u_1(\epsilon; \epsilon^0) + u_2(\epsilon; \epsilon^0)] \quad (17)$$

with

$$u_1(\epsilon; \epsilon^0) = \ln |j - \epsilon \epsilon^0|; \quad (18)$$

$$u_2(\epsilon; \epsilon^0) = \ln \frac{\sinh^{-1} P - \epsilon^2}{\sinh^{-1} P - \epsilon_0^2}; \quad (19)$$

We note that u_1 is translationally invariant in the variables $\epsilon; \epsilon^0$, but u_2 is only invariant in the metallic regime ($\epsilon_0 < 1$). However, in the insulating regime ($\epsilon_0 > 1$) u_2 is negligible compared to u_1 . This fact suggests that we write u_2 for the shifted variables $\epsilon = \epsilon_3; \epsilon^0 = \epsilon_3^0$ as

$$u_2(\epsilon + \epsilon_3; \epsilon^0 + \epsilon_3^0) = u^0(\epsilon; \epsilon^0) + u_2(\epsilon; \epsilon^0; \epsilon_3); \quad (20)$$

where

$$u_2(\epsilon; \epsilon^0; \epsilon_3) = \ln \frac{(\sinh^{-1} P + \epsilon_3)^2}{(\sinh^{-1} P)^2} \frac{(\sinh^{-1} P - \epsilon_0 + \epsilon_3)^2}{(\sinh^{-1} P - \epsilon_0^2)^2}; \quad (21)$$

Then, the integralequation (16) is written as

$$\int_1^{\infty} ds \ln |j \sinh(t-s)j + \ln |j - sj| + \frac{1}{2} u_2(t; s) \rho_{sp}(s) = u(\epsilon + \epsilon_3; \epsilon_1) + u(\epsilon + \epsilon_3; \epsilon_2) \\ + \frac{i}{1 + \epsilon + \epsilon_3} + V(\epsilon + \epsilon_3); \quad (22)$$

where $\rho_{sp}(s)ds = \rho_{sp}(\epsilon + \epsilon_3)d(\epsilon)$ with $\rho_{sp}(\epsilon)d(\epsilon) = \rho_{sp}(x)dx$, while $\sinh^2 t = \epsilon$ and $\sinh^2 s = \epsilon^0$; we have also extended the last integral to negative values since $\rho_{sp}(s) = \rho_{sp}(-s)$. Finally, it turns out that $u_2(t; s)$ can be

approximated by the product of the sum of two Lorentzians whose parameters are determined by the limits $s \rightarrow 0$, $s \rightarrow 1$ and $s \rightarrow 3$. However, a posteriori numerical calculation showed that the contribution to the saddle point free energy $F_{sp}(x_1; x_2; x_3; (x))$ coming from the $u_2(t; s)$ term was negligible. So, in order to simplify our calculations we neglect this term. Our last simplification is related to the interaction terms in $\rho_{sp}(x)$: we consider only interactions between neighboring eigenvalues i.e., $x_1; x_2$ and $x_2; x_3$ and neglect interactions between x_1 and x_3 . As mentioned before, we will check our approximations by comparing $\langle g \rangle$ and $\text{var}(g)$ with those from the model.

Since the right hand side of Eq. (22) is linear in ρ and therefore $\rho_{sp}(s)$, the saddle point free energy (Eq. (14)) is quadratic in ρ , so F_{sp} can be written as

$$F_{sp} = F^0 + (i)F^0 + \frac{(i)^2}{2}F^0 \quad (23)$$

and the integral over ρ in Eq. (15) can be done exactly with the following result:

$$P(g) = \int_0^1 dx_1 \int_{x_1}^1 dx_2 \int_{x_2}^1 dx_3 e^{-S}; \quad (24)$$

where

$$S = \frac{1}{2F^0} (g - F^0)^2 + F^0; \quad (25)$$

Therefore once F_{sp} is obtained from $\rho_{sp}(x)$, the calculation of the distribution $P(g)$ is reduced to a triple integration, Eq. (24), which we compute numerically.

Note that the above described method can in principle be implemented fully numerically, without making approximations on $u_2(t; s)$ or $\rho_{sp}(x)$. The analytic approach allows us to identify the dominant terms and understand their change with disorder. The price we pay is that the expressions for the density and free energy are not valid for all possible values of x_i ($0 < x_i < 1$). In fact, our expressions for $\rho_{sp}(x)$ and F_{sp} are restricted to values of $x_3 < 5$. We will see, however, that it is enough to reach the region of main interest: the crossover regime.

IV. RESULTS AND CONCLUSIONS

We start comparing our calculations to the first two moments available for all degree of disorder from the model [13]. Figure 3 shows that the average and variance of g is now better in the crossover region, compared to the previous calculation of [14], see Fig. 1. On the other hand, the metallic regime is not described as good as in [14] since we have neglected u_2 in Eq. (20) and the interaction terms between x_1 and x_3 . Actually, the approximations made in [14] are quite good in this metallic regime, Fig. 1, and we have included the results (squares) for the average and variance in Fig. 3 for completeness. Similarly, our restriction to values of $x_3 < 5$ for $\rho_{sp}(x)$ does not allow us to go throughout the insulating regime, since in this regime the conductance is dominated by the first two eigenvalues $x_2 \rightarrow x_1 \rightarrow 1$. However, in our approach this region is very well described by two eigenvalues only as the density goes to zero. For completeness, we also include in Fig. 3 the results for such a calculation. Our main goal in this work is to develop approximations that are valid in the crossover region, and as shown in Fig. 3, our current approximations lead to very good results in the desired region. The complete Fig. 3 shows that the two limiting regimes can be described within the same formulation using different set of approximations.

In figure 4 we show the evolution of $P(g)$ as we change the disorder parameter ϵ , evaluated within the current approximations valid in the crossover region. Suppose that we start decreasing the disorder in a sample i.e., we go from insulating to metallic behavior: at $\epsilon = 0.5$ we obtain a broad distribution with a bump at small values of g which is a reminiscence of the huge peak for $g < 1$ in the insulating regime, see Fig. 2. Also, at $g > 1$, $P(g)$ has an exponential decay as has been seen in numerical simulations [6, 7, 8, 9] rather than the Gaussian cutoff at $g > 1$ predicted in [14]. As ϵ is increased ($\epsilon = 0.7$), the bump at $g < 1$ disappears which makes $\langle g \rangle$ increase and at the same time, the decay at $g > 1$ becomes smoother. Finally, when we decrease the disorder even more ($\epsilon = 1.0$), we obtain a distribution which starts to look like a Gaussian distribution, as is expected in the metallic regime.

In order to check our results in the crossover regime, we compare $P(g)$ at $\epsilon = 0.5$ with the distribution obtained numerically by Plerou and Wang [6]. Figure 5 shows a good agreement with the numerical simulation [6], except at $g=1$ where our $P(g)$ has a peak. Others numerical simulations [7, 8, 9, 10] do not show any cusp at $g=1$ either. We believe that this behavior at $g=1$ comes from our restriction $x_3 < 5$ in the density $\rho_{sp}(x)$, since as we go from the metallic to insulating regime large eigenvalues become more and more important. However, this peak eventually develops into the expected peak of the Gaussian in the metallic regime. On the other hand, an essential singularity of $P(g)$ at $g = 1$ has been found in [15] in the crossover regime, on the insulating side. So it is conceivable that the

peak present for $\gamma = 0.5$ due to the existence of this singularity disappears, since the method developed here may not be valid in the presence of such singularities. Also, a non-analytic behavior at $g = 1$ has been found numerically in quasi-one and three-dimensional systems in the crossover regime [10].

In conclusion, we have developed a systematic method which allows us to calculate the distribution of the conductance in a quasi-one-dimensional system. In particular we were interested in the distribution of g across the crossover regime which had not been obtained before [14]. Separating out the two lowest eigenvalues and treating the rest as a continuum in the solution of the DM-PK equation, we were able to obtain the evolution of $P(g)$ as function of the disorder parameter γ . We have shown how $P(g)$ develops from a broad flat distribution at the crossover regime to a Gaussian distribution in the metallic regime. Our results for the average and variance agree with the exact results from the non-linear sigma model and the distribution $P(g)$ in the crossover regime agrees well with the numerical calculation [6], including an exponential decay for $g > 1$ reported in numerical simulations. Together with the earlier results of how a log-normal distribution on the insulating side develops a cutoff at $g = 1$ and eventually becomes an asymmetric 'one-sided' log-normal distribution near the crossover regime, this provides a relatively complete picture of how a log-normal distribution becomes a Gaussian via a highly asymmetric intermediate one-sided log-normal distributions when disorder is changed. The quantitative details at $g = 1$ at the crossover point remain an open question.

Although our results are valid strictly only for quasi-one-dimensional systems where the DM-PK equation is valid (however, it has been shown that the restriction $L \ll W$ can be relaxed [18]), a qualitatively similar behavior of $P(g)$ is found numerically in 2 and 3 dimensional systems in the crossover regime [7, 10]. It is therefore possible that the method presented here could help understanding the generic behavior in higher dimensions at the crossover regime.

Acknowledgments

We are grateful to Ziqiang Wang for sharing his results for the distribution of the conductance in the crossover regime. One of the authors (V.A.G.) acknowledges financial support from CONACYT, Mexico. K.A.M. is grateful for hospitality at the University of Karlsruhe and acknowledges support from SFB 195 of the DFG. P.W. acknowledges support through a Max-Planck Research Award.

-
- [1] Mesoscopic Phenomena in Solids, edited by B.L. Altshuler, P.A. Lee and R.A. Webb, Elsevier, Amsterdam 1991; C.W.J. Beenakker, Rev. Mod. Phys. 69, 731 (1997).
 - [2] Supriyo Datta, Electronic Transport in Mesoscopic Systems, Cambridge University Press 1995.
 - [3] S.W. Ashburn and R.A. Webb, Adv. Phys. 35, 375 (1986).
 - [4] P. Mohanty and R.A. Webb, Phys. Rev. Lett. 88, 146601 (2002).
 - [5] B.L. Altshuler, Pis'ma Zh. Eksp. Teor. Fiz. 41, 530 (1985); P.A. Lee and A.D. Stone, Phys. Rev. Lett. 55, 1622 (1985).
 - [6] V. Plerou and Z. Wang, Phys. Rev. B 58, 1967 (1998).
 - [7] P. Markos, Phys. Rev. Lett. 83, 588 (1999).
 - [8] M. Rühlander and C.M. Soukoulis, Physica B Cond. Matt. 296, 32 (2001).
 - [9] M. Rühlander, P. Markos and C.M. Soukoulis, Phys. Rev. B 64, 212202 (2001).
 - [10] P. Markos, Phys. Rev. B 65, 104207 (2002).
 - [11] A. Garcia-Martin and J.J. Saenz, Phys. Rev. Lett. 87, 116603 (2001).
 - [12] M.R. Zimbauer, Phys. Rev. Lett. 69 (1992).
 - [13] A.D. Mirlin, A.M. Ulloa-Groeling and M.R. Zimbauer, Ann. Phys. (N.Y.) 236, 325 (1994).
 - [14] K.A. Muttalib and P. Woelke, Phys. Rev. Lett. 83, 3013 (1999); P. Woelke and K.A. Muttalib, Ann. Phys. (Leipzig) 8, 753 (1999).
 - [15] K.A. Muttalib, P. Woelke, A. Garcia-Martin and V.A. Gopar (unpublished).
 - [16] O.N. Dorokhov, JETP Lett. 36, 318 (1982); P.A. Mello, P. Pereyra and N. Kumar, Ann. Phys. (N.Y.) 181, 290 (1998).
 - [17] C.W.J. Beenakker and B. Rejaei, Phys. Rev. Lett. 71, 3689 (1993); C.W.J. Beenakker and B. Rejaei, Phys. Rev. B 49, 7499 (1994).
 - [18] C.W.J. Beenakker and J.A.M.elsen, Phys. Rev. B 50, 2450 (1994).

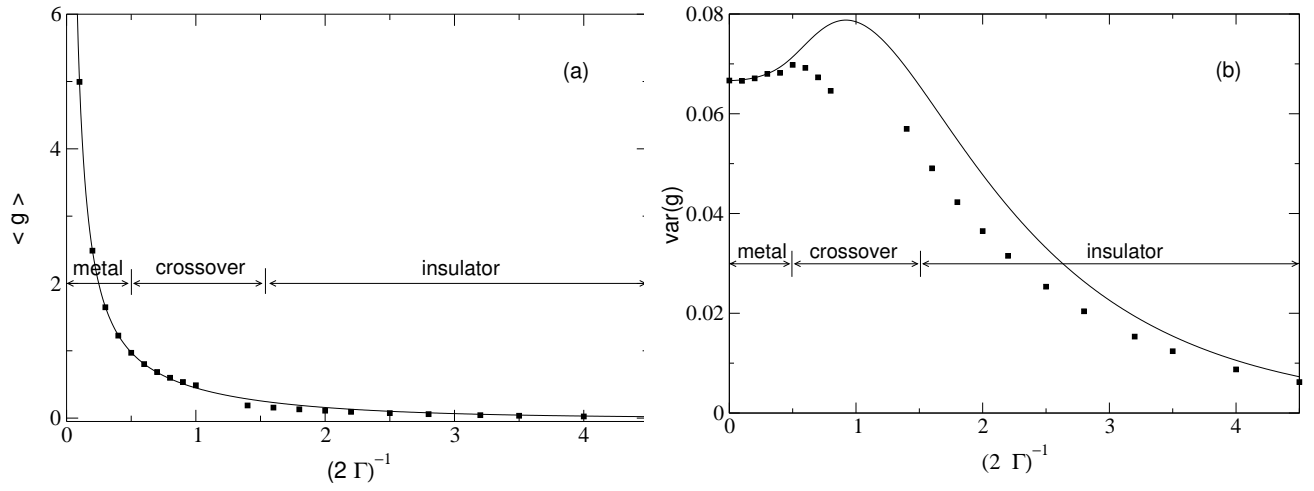


FIG. 1: (a) Mean and (b) variance of g calculated from the results in [14] (squares) are compared with the correspondent results from the model (solid line) [13]. Horizontal arrows show schematically the different regimes of transport. Note that $\langle g \rangle$ and $\text{var}(g)$ from [14] are not calculated for the complete crossover region, since the deviation from the model results becomes large.

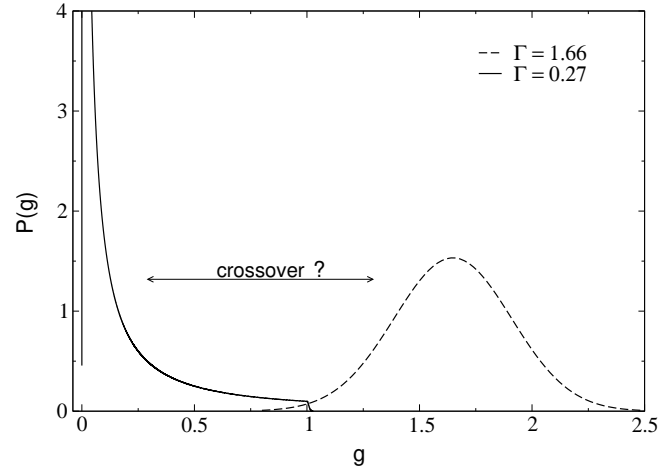


FIG. 2: Distribution $P(g)$ in the metal (dashed line) and insulating (solid line) regime calculated by using the results in [14]. As expected, a Gaussian distribution is obtained for the metallic case while, in a logarithmic scale, $P(\ln g)$ follows a log-normal distribution for the insulating case.

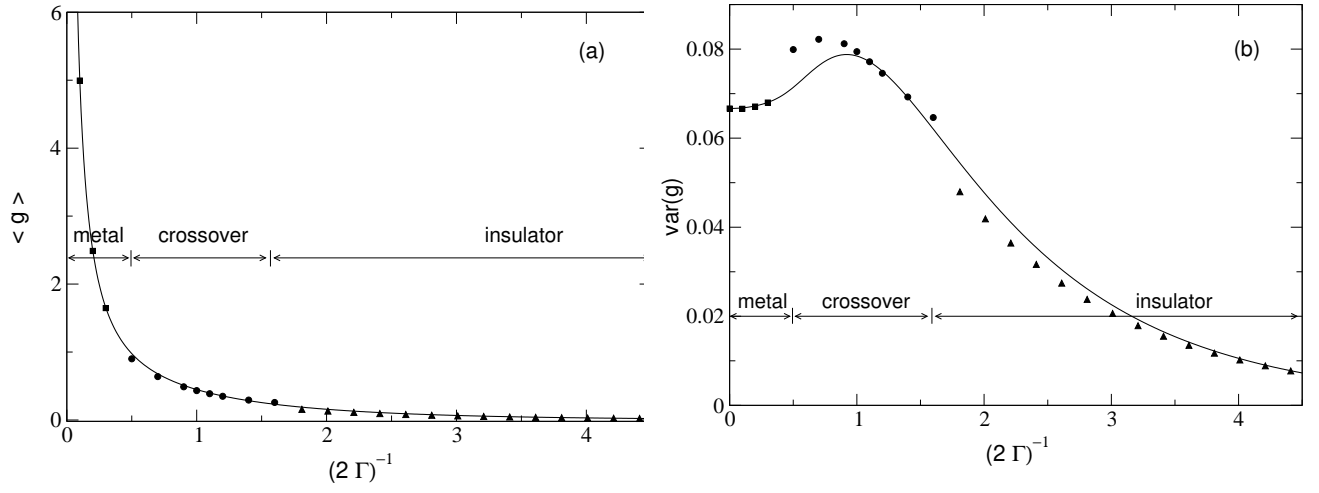


FIG. 3: Comparison of our results for the average and variance of the conductance, (a) and (b) respectively, with the non linear model (solid line) [13]. Squares are the same as in Fig. 1. Dots are results obtained using the current approximations for the crossover region. Triangles are results obtained using two eigenvalues only.

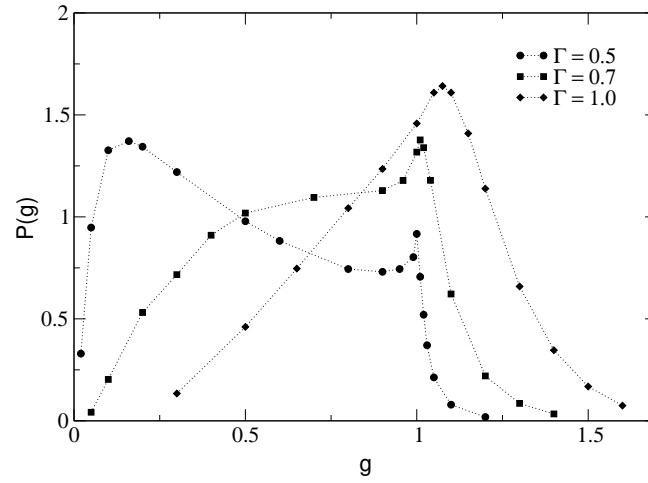


FIG. 4: Evolution of the distribution of the conductance $P(g)$ as the disorder parameter Γ is changed. Three cases are shown $\Gamma = 0.5$ (dots), $\Gamma = 0.7$ (squares) and $\Gamma = 1.0$ (diamonds).

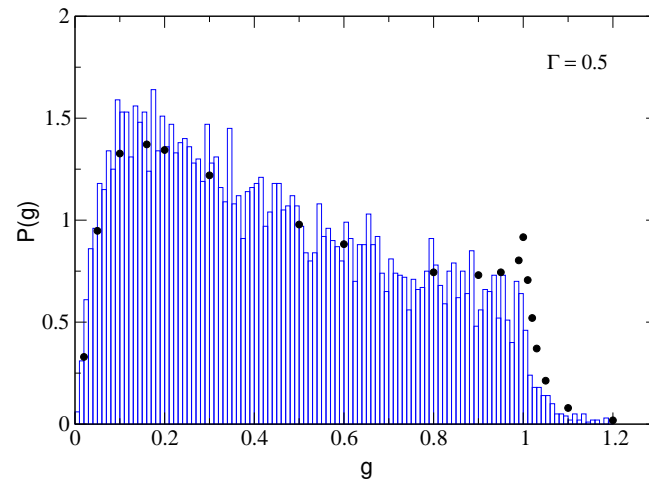


FIG. 5: Comparison of our result for the distribution of g at $\Gamma = 0.5$ (dots) with the numerical calculation presented in [6] (bars).